JOURNAL OF GEOPHYSICAL RESEARCH, VOL. 111, C09S90, doi:10.1029/2005JC003179, 2006

Physical-biological interactions in North Pacific oxygen variability

Curtis Deutsch,[1] Steven Emerson,[1] and LuAnne Thompson[1]

Received 20 July 2005; revised 22 November 2005; accepted 2 May 2006; published 8 September 2006.

[1] We investigate the temporal variability of oxygen in the upper water column of the North Pacific using a hindcast ocean model. The model embeds simple biogeochemical cycles of nutrients and O_2 within an isopycnal circulation model that is forced at the surface by historical atmospheric conditions. The resulting O_2 variability is spatially and temporally complex, but includes large-scale O_2 decreases between the 1980s and 1990s in the subpolar region, and simultaneous O_2 increases in the subtropics. These simulated changes are similar in pattern to those observed along repeat transects (Emerson et al., 2004), suggesting that the model captures key mechanisms of late twentieth century O_2 variability in the North Pacific. Additional simulations were performed to distinguish O_2 changes due to variability in biology, ventilation, and circulation. Regional trends in export production drive significant oxygen changes that are focused in the upper thermocline, where remineralization rates are largest. However, shallow biological O_2 changes are often balanced by opposing physically driven O_2 changes. In contrast, physical processes of ventilation and circulation are found to be the dominant cause of model O_2 variability in the lower ventilated thermocline, where observed O_2 anomalies are the largest. These results suggest that O_2 variability in the lower ventilated thermocline may be a useful tracer of physical climate change in the North Pacific, while changes in the biological pump may be difficult to detect on the basis of O_2 trends alone. Continued analysis of historical patterns of subsurface O_2 variability will provide important further tests of these conclusions.

Citation: Deutsch, C., S. Emerson, and L. Thompson (2006), Physical-biological interactions in North Pacific oxygen variability, *J. Geophys. Res.*, *111*, C09S90, doi:10.1029/2005JC003179.

1. Introduction

[2] Understanding the response of the biological productivity and circulation of the oceans to anthropogenic climate change poses an enormous challenge with broad implications for the global carbon cycle. Historical ocean observations document the impact of recent climate change, both natural and anthropogenic, and offer unique opportunities to test and advance our understanding of fundamental physical-biogeochemical ocean processes. No oceanic parameter that records both biological and physical processes has been measured as accurately and with as dense a temporal and spatial coverage as dissolved oxygen gas (O_2). Analysis of historical oxygen data has revealed significant changes in oxygen concentrations in the thermocline of most ocean basins over the past few decades [*Bindoff and McDougall*, 2000; *Emerson et al.*, 2001; *Garcia et al.*, 1998; *Johnson and Gruber*, 2006; *Keller et al.*, 2002; *Matear et al.*, 2000; *Ono et al.*, 2001; *Shaffer et al.*, 2000; *Watanabe et al.*, 2001]. These observations provide important constraints on late twentieth century changes in both the biological and physical processes controlling the oceanic O_2 distribution, and may yield clues to the recent past and potential future of oceanic CO_2 uptake.

[3] At any given point in the ocean interior, variations in O_2 through time reflect imbalances between the biological consumption of O_2 during the respiration of organic matter and its physical supply via the transport of O_2-rich surface waters. An increase in the organic matter exported to depth and/or the fraction of that export flux being oxidized at a given depth or density surface will increase the rate of O_2 consumption on that surface, causing O_2 concentrations to decline. An increase in the flux of O_2-rich surface waters into the permanent thermocline (hereafter ''ventilation'') or the rate at which newly ventilated waters are circulated through the interior will increase the O_2 content. Finally, thermocline O_2 concentrations can also be altered at the sea surface by changes in the thermodynamically saturated O_2 concentration, O_2^{sat}, or in the degree of equilibration attained through gas-exchange with the atmosphere [*Ito et al.*, 2004]. The net effect of biology, ventilation, and circulation on O_2 concentrations is represented by Apparent Oxygen Utilization (AOU), defined as the local O_2 deficit relative to its saturated value ($AOU = O_2^{sat} - O_2$).

[4] While differences in O_2 concentrations between decades have been detected in nearly every ocean basin, changes in the North Pacific are the most extensively analyzed and documented (see review by *Emerson et al.* [2004]). Comparison of O_2 data collected along three trans-

[1]School of Oceanography, University of Washington, Seattle, Washington, USA.

0148-0227/06/2005JC003179$09.00

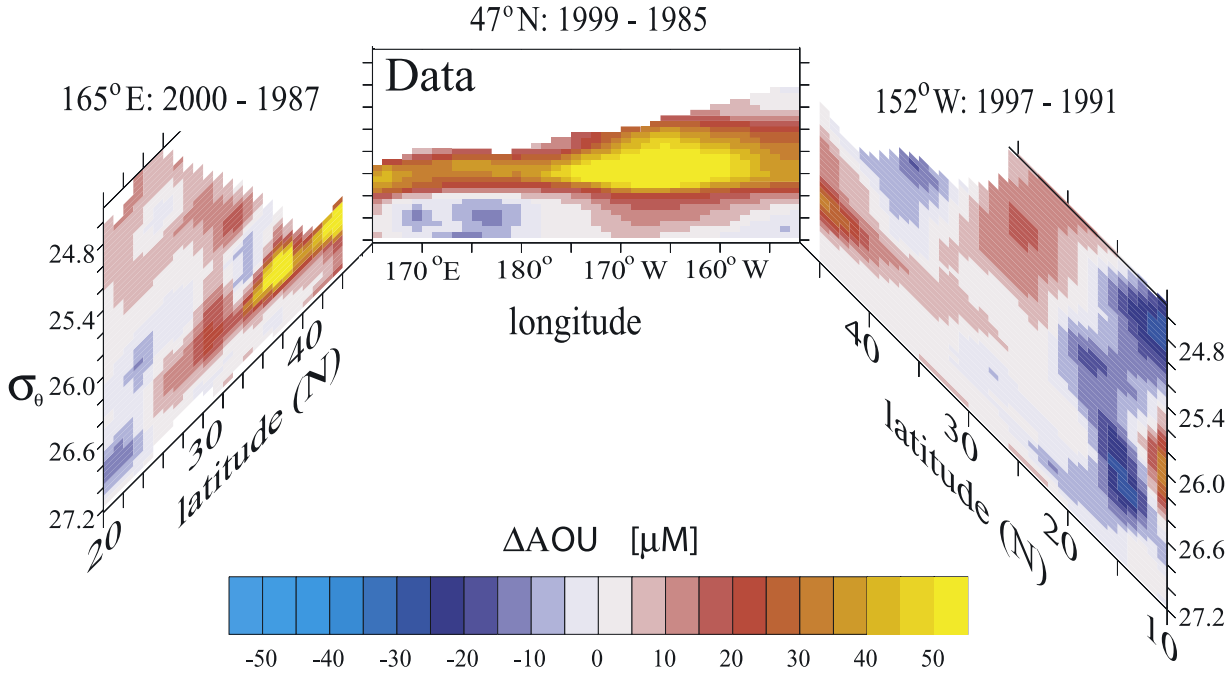

Figure 1. AOU difference (μmol/kg) between measurements made during different years from 1985 to 2000 along three sections through the North Pacific. Data sources are as referenced by *Emerson et al.* [2001, 2004]. Sections are mapped for each cruise at regular intervals of potential density (σ_θ) using a "loess" interpolation and then subtracted as $AOU_{later} - AOU_{earlier}$. Only waters below the wintertime outcrop are plotted.

ects through the North Pacific reveal large O_2 differences, between cruises that occurred in the 1980s and again in the 1990s (Figure 1) although high frequency variability (seasonal and shorter) may contribute to O_2 differences between cruises, the large-scale pattern of O_2 changes appears to be decadal in nature, as discussed below and is dominated by AOU with only small changes in O_2^{sat}. Over much of the midlatitude North Pacific (~20°N–50°N), AOU rose by 10–80 μM, with the largest increases in the subtropical/subpolar boundary and at the base of the ventilated thermocline, in the densest waters that currently outcrop in the open Subarctic Pacific ($\sigma_\theta \sim 26.6$). In the northern subtropics from ~25°N to 30°N, AOU increases are also observed, but with smaller magnitudes of ~10–20 μM. Below the directly ventilated thermocline ($\sigma_\theta > 26.8$), AOU appears to have undergone little change in these regions, or perhaps a slight decrease [*Keller et al.*, 2002]. Finally, at the southern edge of the region examined by *Emerson et al.* [2004], O_2 increases appear to have occurred between the 1980s and 1990s.

[5] Several potential sources of physical and biological variability could contribute to the observed O_2 changes. Variability in the physical conditions of the North Pacific is a prominent feature of the global climate system. Sea surface temperature (SST) exhibits large-scale anomaly patterns that evolve on timescales of years (El Niño/ENSO), as well as decades (Pacific Decadal Oscillation, or PDO). Midlatitude SST anomalies have been shown to propagate into the ventilated thermocline, providing a direct, albeit lagged link between surface and thermocline variability [*Deser et al.*, 1996]. While the direct effect of temperature variability on thermocline O_2 is small (typical thermocline temperature anomalies of <1°C yield changes in O_2^{sat} of <5 μmol/kg), it can also influence AOU by modifying the rate of O_2 exchange between the mixed layer and the ocean interior, and its transport within the thermocline. For example, the PDO has been linked to changes in mixed layer depth in the subtropical/subpolar transition zone [*Polovina et al.*, 1995] and the intensity of the Kuroshio current [*Deser et al.*, 1999].

[6] Changes in the marine biosphere of the North Pacific have also been observed over the last several decades. Measurements from the Hawaii Ocean Time Series station indicate that biological productivity in the subtropical gyre increased between the 1980s and 1990s [*Karl et al.*, 1997]. Chlorophyll data extending back to the 1960s suggests that the productivity increase may have begun even earlier [*Venrick et al.*, 1987]. Evidence from higher trophic levels also shows large-scale ecological oscillations in the past several decades [*Chavez et al.*, 2003]. Several of these biological trends appear to be associated with transitions in physical climate indices, although the mechanisms are not understood.

[7] Attributing the causes of O_2 change from observations alone is a difficult task, since O_2 concentrations in the ocean interior integrate the effects of several processes over timescales of years to decades. A local O_2 anomaly may be produced by biological or physical processes acting in

isolation or in combination and may persist long enough to be transported far from the region of origin. Processes capable of altering the distribution of subsurface O_2 are not wholly independent however. First, ventilation and circulation changes are dynamically linked. A change in ventilation will perturb the local circulation and redistribute the ventilation-induced O_2 anomaly, and an altered circulation may affect the location and/or rates of thermocline ventilation. Second, the close coupling of nutrient and oxygen cycles in the ocean requires that changes in the physical O_2 supply be compensated to some degree by changes in biological O_2 consumption. An increase in the O_2 transported to the interior owing to more vigorous circulation/ventilation rates must be balanced by an increase in the flux of nutrients back to the surface. Assuming a constant surface nutrient reservoir, organic matter export and the associated subsurface O_2 demand must also increase, counteracting the increased O_2 supply. Although this biological compensation acts to dampen changes in basin-scale O_2 inventory, imbalances between O_2 supply and demand are possible regionally, and for periods shorter than the decadal timescale of thermocline ventilation.

[8] Accounting for the interactions between physical and biological processes driving O_2 variability across different regions and time periods in the North Pacific requires a numerical general circulation/biogeochemistry model capable of resolving the spatial and temporal scales of observed O_2 changes and its potential causes. The goal of this paper is to characterize and attribute O_2 variability in the North Pacific using a hindcast model that simulates changes in both physical and biological O_2 fluxes. The model simulations presented here have been used previously to argue that the large O_2 changes observed in the lower ventilated thermocline are primarily physical in origin [*Deutsch et al.*, 2005]. Here we place those results in a wider context by exploring the relationships (1) between physically and biologically driven O_2 variability, (2) between O_2 variability at different depths of the upper water column and across different regions of the basin, and (3) between features of simulated O_2 variability caused by transient perturbations versus longer-term trends in the physical circulation of the North Pacific. We note however, that the climate-forced variability of oceanic O_2 cannot resolve the nature or causes of the climate trends or distinguish between anthropogenic and natural climate variability.

[9] In the following section, we describe the model used to simulate O_2 changes in the North Pacific from 1948 to 2000. In section 3 we present model results and compare them to the data compiled by *Emerson et al.* [2004]. In section 4, the character and causes of O_2 variability in different regions of the North Pacific is discussed, permitting a mechanistic examination of regional O_2 changes and the basin-wide O_2 balance. A brief summary discussion and conclusions are given in section 5.

2. Model

[10] In this section, we describe the physical model used to simulate changes in O_2 supply, as well as a simple model of the biological pump, which allows us to estimate variability in O_2 demand arising from changes in biological export production.

[11] Ocean circulation is computed using a version of the Hallberg Isopycnal Model (HIM) [*Hallberg and Rhines*, 1996; *Ladd and Thompson*, 2001] that is configured for a North Pacific domain from 20°S to 60°N. The basin is resolved on a 1° grid with 14 isopycnal layers and a Kraus-Turner mixed layer with spatially variable density. The interaction between isopycnal layers and the mixed layer is mediated by an additional buffer layer, through which winter mixed layer water is transferred onto isopycnal surfaces in the permanent thermocline. Ocean circulation fields are forced at the surface by prescribed atmospheric conditions including wind stress and heat flux computed using surface air temperature and bulk formulae. Sea surface salinity is restored toward its climatological distribution [*Levitus and Boyer*, 1994]. The circulation is first time stepped forward to steady state using climatological forcing, and then integrated an additional 52 years using interannually varying atmospheric winds and surface air temperatures from NCEP reanalyses between 1948 and 2000 [*Kalnay et al.*, 1996]. Changes in surface fresh water flux (E-P) are not included in the variable forcing. Aspects of model circulation variability have been investigated by *Thompson and Ladd* [2004].

[12] Time-dependent tracer distributions are computed in an offline advection/diffusion routine using monthly averaged circulation fields from the GCM, following the strategy of *McKinley et al.* [2004]. The distribution of four tracers is determined: phosphate (PO_4), dissolved organic phosphorus (DOP), O_2, and ideal age. DOP and PO_4 are used to diagnose O_2 fluxes associated with the biological pump (see below), and ideal age is computed to provide a measure of the time elapsed since a water parcel was last at the surface [*Thiele and Sarmiento*, 1990]. All tracers are diffused along isopycnal surfaces using an eddy diffusion coefficient of 2000 m^2/s [*Jenkins*, 1990]. Diapycnal mass fluxes include a diffusive flux based on a constant diapycnal diffusivity of 0.1 cm^2/s [*Ledwell et al.*, 1993]. Within 5° of the open boundaries of the model domain, PO_4 and O_2 are restored toward annual mean values [*Conkright et al.*, 1994]. We integrate all tracer distributions to a near-steady state (300 years) using annually recurring, monthly circulation fields. Steady state tracer distributions are then used as initial conditions for a simulation using the variable circulation derived from historical atmospheric forcing (1948–2000).

[13] The sources and sinks of biogeochemical tracers are computed using parameterizations based on the Ocean Carbon Model Intercomparison Project (OCMIP) [*Najjar and Orr*, 1999]. In the OCMIP protocol, biological organic matter production is diagnosed by restoring model PO_4 toward climatological values in the upper 75 m, with a restoring timescale of 30 days. Of the total organic matter production, two thirds is converted to DOP, which is advected and diffused and decays back to PO_4 with a half-life of 1 year. The remaining one third is exported as sinking flux, which is instantly remineralized to PO_4 at depth with an effective length scale of ~300 m. The production and remineralization of organic phosphorus pools produces and consumes O_2 in a constant stoichiometric O_2:P ratio of −170 mol O_2/mol P [*Anderson and Sarmiento*, 1994], except in suboxic waters ($O_2 < 4$ umol/kg) where O_2 consumption ceases. Mixed layer O_2 concentrations are

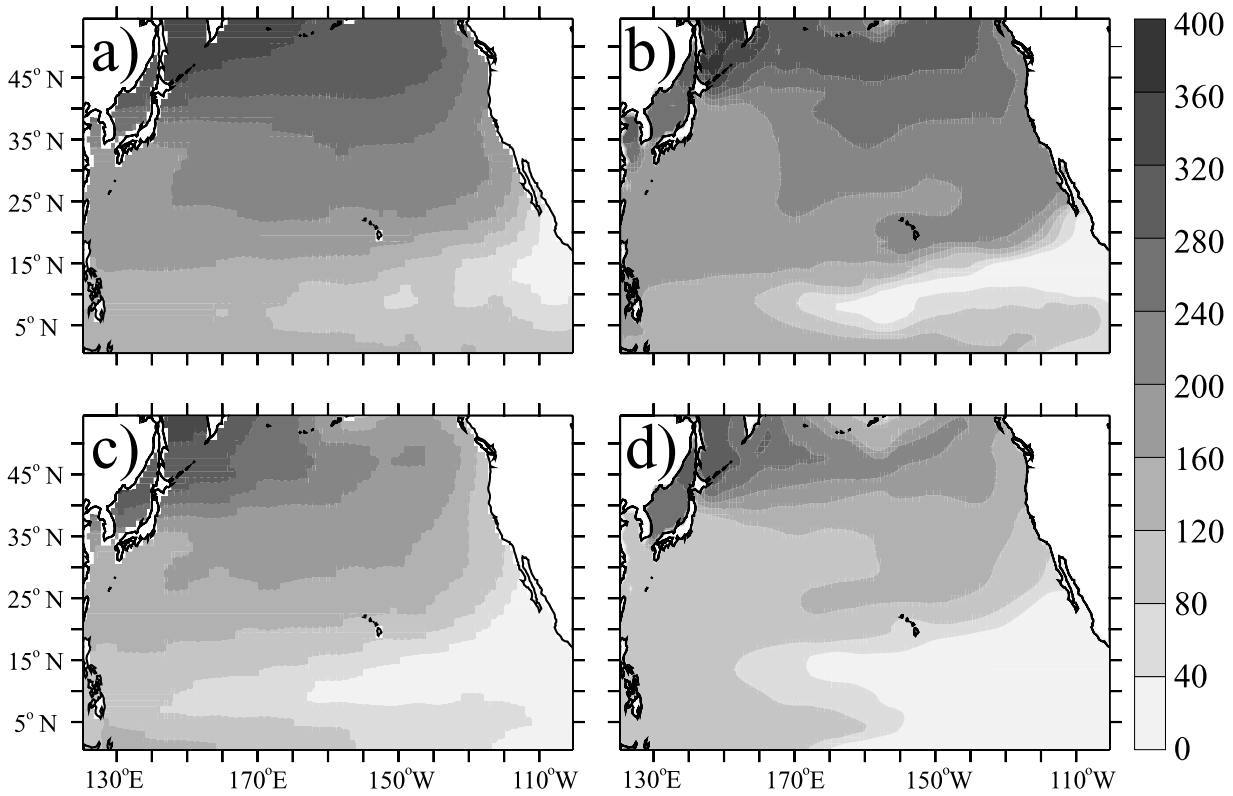

Figure 2. Annual mean O_2 concentration (μmol/kg) from (a, c) climatological observations and (b, d) steady state model simulation for two isopycnal surfaces: σ_θ 25.8 (Figures 2a and 2b), which lies within the Central Mode Water, and σ_θ 26.6 (Figures 2c and 2d), which lies at the base of the ventilated thermocline.

fixed at their time-varying thermodynamically saturated values.

[14] The surface PO_4 fields used to compute organic matter export are constant throughout the simulation; however, export flux diagnosed through nutrient restoring can vary owing to changes in nutrient supply. If the supply of PO_4 to surface waters increases, biological production must also increase in order to maintain constant observed surface PO_4 concentrations. This parameterization of the biological pump therefore represents only those biological changes that are associated with changes in nutrient supply. It is possible that changes in biological export production over the past few decades also resulted in a net change in surface nutrient distributions. Since little is known about whether surface nutrient distributions changed over the late twentieth century, we make the tentative assumption that they have not. In regions where surface PO_4 concentrations have declined, our model will underestimate the influence of biological changes on O_2, whereas it will overestimate changes in subsurface O_2 in regions where surface PO_4 has increased.

3. Results

[15] Here we present the model's mean O_2 distribution and its changes through time from 1948 to 2000, with a focus on differences between the 1980s and the 1990s, in the region between 20°N and 50°N, where observed O_2 changes have been reviewed by *Emerson et al.* [2004]. Results from the isopycnal surface σ_θ 26.6, where observed O_2 changes are largest in magnitude, are contrasted with changes from a shallower density layer, σ_θ 25.8 that lies within the Central Mode Water (CMW). Because the isopycnal σ_θ 26.6 includes the deepest waters that typically outcrop in the open North Pacific in both the model and the real ocean [*Levitus and Boyer*, 1994], we refer to this layer as the lower ventilated thermocline. We neglect model O_2 changes in the tropics, and prior to 1970, since such changes are not documented in the literature.

3.1. Climatological Mean State

[16] Simulating a realistic mean O_2 distribution is an important precondition for simulating realistic temporal O_2 changes. Biases in a model's mean O_2 distribution can lead to biases in O_2 changes through time. For example, if an O_2 gradient is too strong in the climatological mean state, the displacement of any current associated with that gradient will produce local O_2 changes that are unrealistically large. Of course, no model will exactly reproduce the observed O_2 distribution, but understanding errors in the mean O_2 distribution helps calibrate ones confidence in various features of the simulated O_2 variability.

[17] The observed large-scale distribution of O_2 in the thermocline of the North Pacific is reproduced by our isopycnal model (Figure 2). Annual mean model O_2 concentrations throughout the ventilated thermocline are high in the northwest Pacific, where these water masses outcrop in winter, decreasing to low values in the eastern tropical

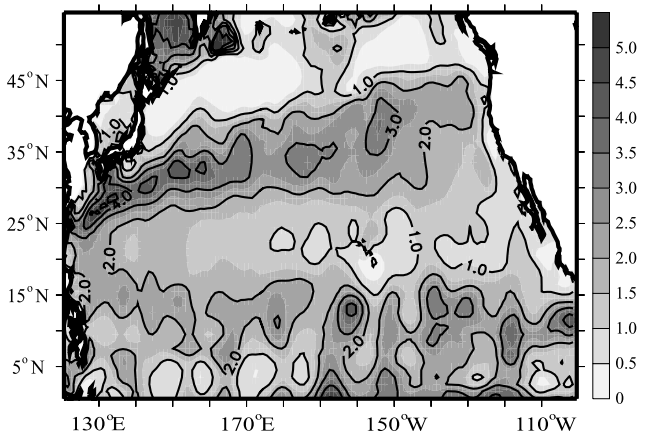

Figure 3. Steady state export production (mol C/m^2/yr) diagnosed from surface PO_4 restoring, assuming a C:P ratio of 117:1. Export production is proportional to the oxygen utilization rate (OUR) integrated over the water column.

Pacific where waters are far from regions of ventilation and have therefore undergone a large degree of O_2 consumption. On σ_θ 25.8, the model's oxygen minimum zone in the eastern tropical Pacific is larger than observed, extending too far equatorward along the North American coast, and too far west along 10°N. Model O_2 gradients along the southeastern boundary of the subtropical gyre and across the Kuroshio Extension on this density surface are stronger than in the climatology. In the lower thermocline (σ_θ 26.6), O_2 gradients in these regions are similar to observations, but overall O_2 is slightly low.

[18] Total O_2 consumption integrated over the water column from the depth of organic matter export (75 m) to the bottom is equal to the export of organic matter (Figure 3). The model concentrates export production in the regions of upwelling and at gyre boundaries. Productivity is lower than suggested by observational estimates at ocean time series sites in the subtropical and subpolar gyres [*Emerson et al.*, 1995; *Wong et al.*, 1999b], indicating that nutrient supply is too weak, possibly owing to the model's low diapycnal diffusivity and/or the absence of mesoscale eddies [*McGillicuddy et al.*, 1999]. Overall, however, the agreement between simulated steady state O_2 distributions and observed climatological values suggests that the physical supply of and biological demand for O_2 in the North Pacific thermocline are adequately represented in the model.

3.2. Interdecadal Variability

[19] When forced by historical atmospheric conditions, model O_2 distributions exhibit significant variability throughout much of the North Pacific thermocline. In order to assess the fidelity of simulated O_2 variability, we compare observed AOU differences between cruises occurring along similar transects in the 1980s and the 1990s [*Emerson et al.*, 2004] to model output from the same transects and years. In both cases, O_2 differences have been analyzed with density rather than depth, as a vertical coordinate [*Lozier et al.*, 1994]. This choice emerges naturally from the model structure, but is primarily motivated by the desire to avoid the appearance of observed O_2 changes in depth coordinates that result from a shift in the depth of key water masses.

[20] Because we are interested in O_2 variability at interannual and longer timescales, we base our comparison on annual mean model O_2 concentrations. Observed O_2 differences however, are based on measurements made during different months as well as different years. Attempts to identify biases in data comparisons are described by *Emerson et al.* [2004] and in Appendix A. The contribution of seasonal variability to the observed O_2 changes, especially along the subpolar section (47°N), can be significant locally but is unlikely to produce the coherent basin-wide change observed. Furthermore, the O_2 decreases observed at the northern edges of the meridional transects match quite well the differences observed at nearby locations in the zonal transect, despite the fact that the seasons sampled on each line were different. In the data/model comparison we emphasize the pattern of O_2 changes, recognizing that local O_2 differences may reflect a seasonal cycle superimposed on longer term changes.

[21] Across most of the subpolar section (47°N), from the base of the mixed layer to the bottom of the ventilated thermocline (σ_θ 26.8), model AOU increases by 5–30 μM between cruise dates 1985 and 1999 (Figure 4). Increases are most pronounced along σ_θ 26.6, becoming weaker above and below that isopycnal. Below the directly ventilated layers ($\sigma_\theta > 26.8$), AOU undergoes a slight overall decrease, consistent with *Keller et al.* [1999]. Modeled AOU differences between these years are qualitatively similar to those found in the observations, although the model underestimates the magnitude of observed O_2 changes in some areas by a factor of 2–3.

[22] The vertical structure of AOU differences along 47°N persists into the northern subtropics, where maximum AOU increases are bounded above ($\sigma_\theta < 26.0$) and below ($\sigma_\theta > 26.8$) by anomalies that are close to zero. In the eastern section, model AOU changes reverse sign in the subtropical gyre, where AOU decreases (O_2 increases) are simulated throughout the water column south of 20°N. In the data compilation of *Emerson et al.* [2004], the eastern transect included cruises from 1984 and 1997 (Marathon and STUD97, respectively) that are suggestive of a similar change. However, the Marathon cruise only went to 25°N and therefore only captured the very edge of the temporal AOU decrease. For our comparison, we have replaced this earlier cruise by the WOCE P16 line (November 1991), since it revealed similar O_2 changes, but contained O_2 data as far south as 10°N.

[23] The overall patterns of simulated O_2 variability between the 1980s and 1990s bear a strong resemblance to observed changes. Most of the features in the observed AOU difference sections can also be identified in model results although, as noted, the magnitude of AOU differences across this time period is generally underestimated, especially along 47°N. On the strength of the similarity in spatial pattern of observed and simulated AOU changes, we expand the investigation of model O_2 variability beyond the years and transects provided by historical data analysis. We discuss the remaining results in terms of O_2 rather than AOU changes, although the two quantities are everywhere nearly equal and opposite, since ΔO_2^{sat} is negligible.

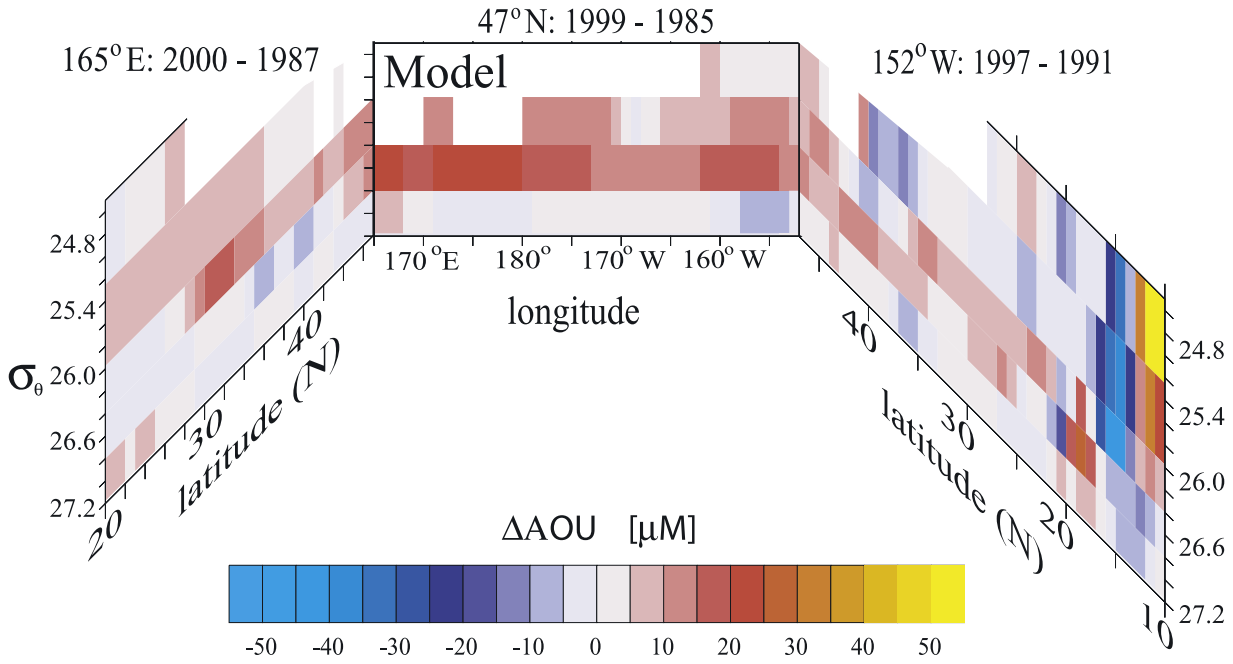

Figure 4. Simulated annual mean AOU differences from the same transects and years as in the observations (see Figure 1). Values poleward of the wintertime outcrop are not shown.

[24] Decadal O_2 changes seen along individual model sections reflect large-scale regional changes on isopycnal surfaces (Figures 5a and 5c). In particular, the O_2 decrease between 1985 and 2000 in the lower ventilated thermocline (σ_θ 26.6) along 47°N is part of a large-scale decrease from the 1980s to 1990s throughout most of the subpolar gyre. Similarly, the subtropical O_2 increases indicated by meridional sections reflect decadal changes extending across the basin throughout the water column. Thus O_2 changes observed during individual years on individual transects appear to be representative of broad basin- and decadal-scale O_2 changes.

[25] While coherent large-scale changes can be identified between the 1980s and 1990s, these changes do not necessarily represent longer-term trends. Outside the subpolar region, O_2 differences between the 1970s and 1980s (Figures 5b and 5d) bear little resemblance to subsequent changes into the 1990s (Figures 5a and 5c). In the eastern subtropics, decreases from the 1980s to the 1990s were preceded by increases from the 1970s to the 1980s. Similarly, part of the O_2 increase in the central gyre in the latter decade was preceded by an earlier O_2 decrease. The change in magnitude and sign of subtropical O_2 variations from the 1970s to the 1990s indicates that many of the observed O_2 changes between the 1980s and 1990s are best interpreted as transient anomalies rather than multidecadal trends. In contrast, the subpolar O_2 decreases are sustained from the 1970s through the 1990s, although the magnitudes change.

[26] Insight into the role of physical processes that affect simulated O_2 changes can be gained by examining contemporaneous changes in ideal age. Enhanced ventilation increases the input of young, O_2-rich waters into the ocean interior, causing a simultaneous reduction in ideal age and increase in O_2. A decrease in ventilation would also produce age and O_2 anomalies of the opposite sign (positive for age and negative for O_2). An intensified circulation would also cause a water mass to be younger and better oxygenated than it would be under a more sluggish circulation, and vice versa. Therefore changes in ventilation and circulation should each produce O_2 and age anomalies that are negatively correlated. In contrast, thermocline O_2 anomalies caused by changes in biological export from surface waters need not be related to the age of the underlying thermocline. Patterns of O_2 change throughout the simulation are correlated to changes in ideal age on both isopycnal surfaces (Figures 6a and 6b). Regions that exhibit increases in ideal age exhibit reduced O_2 (e.g., the tropics, subpolar region on σ_θ 26.6) while decreased age is accompanied by increased O_2 (e.g., the subtropical gyre). The decrease in ideal age in the eastern subtropical Pacific is consistent with decreased pCFC ages reported by *Mecking et al.* [2006]. That such correlations are observed in the model suggests that the direct affects of circulation and ventilation changes are an important cause of O_2 variability.

[27] Changes in the circulation and ventilation of the North Pacific thermocline cannot however, be the sole cause of simulated O_2 anomalies. Water mass transport and mixed layer–thermocline exchange also affect the supply of nutrients to surface waters, producing significant large-scale changes in the diagnosed export of organic matter (Figure 7). Export production increases from the 1980s to the 1990s in a band extending across the tropics,

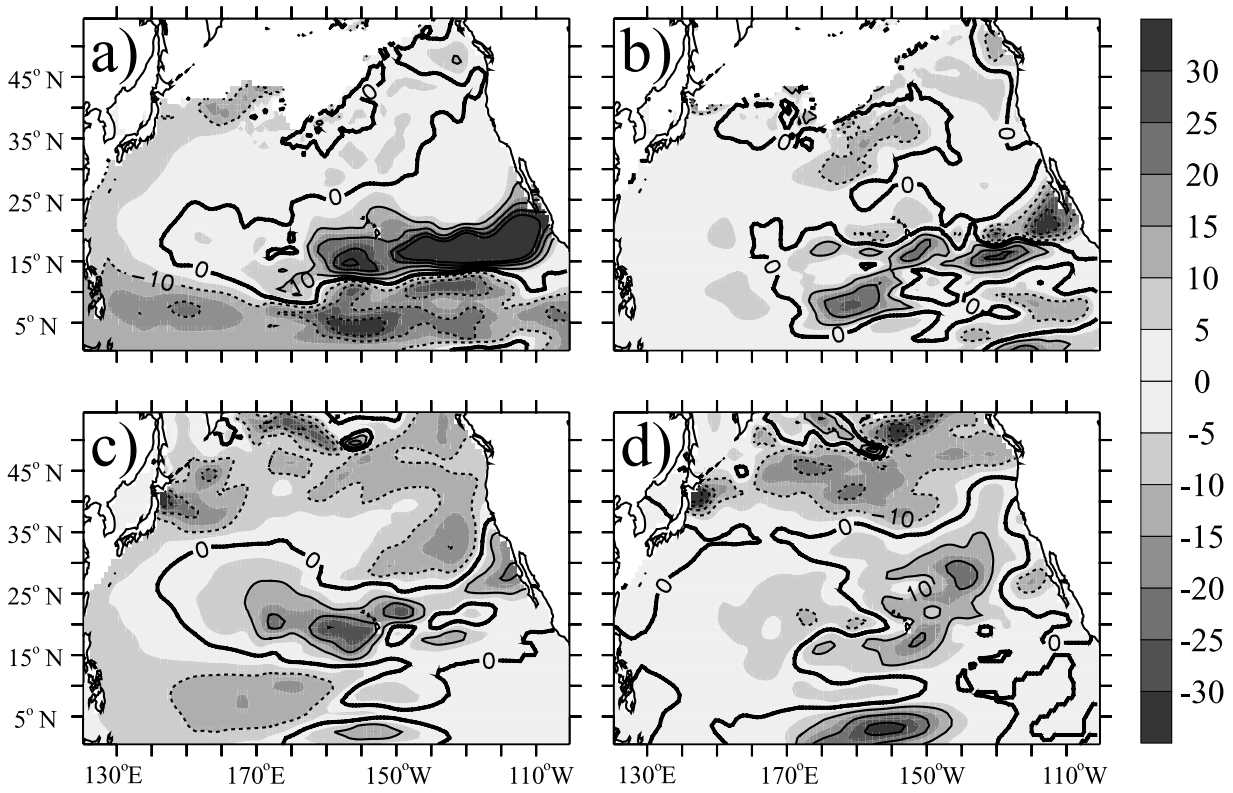

Figure 5. Change in decadal mean O_2 concentrations (μmol/kg) from (a, c,) the 1980s to the 1990s and (b, d) the 1970s to the 1980s for isopycnal layers σ_θ 25.8 (Figures 5a and 5b) and σ_θ 26.6 (Figures 5c and 5d) (see Figure 2 for layer definitions). Positive values indicate increasing O_2 (decreasing AOU) with time.

north along the western boundary, and toward the east in the subtropical/subpolar transition zone. Decreased export is simulated in a band stretching across the eastern tropics from ~15°N to ~25°N. With the exception of the central North Pacific, the primary export production changes appear to be related to the O_2 anomalies on σ_θ 25.8 (see Figure 5). The relationship appears much weaker however, in the lower ventilated thermocline.

[28] In summary, simulated O_2 changes over the 1980s–1990s are similar in pattern to observed changes, although the magnitude of variations is underestimated by the model. This spatial similarity suggests that the model captures the first-order processes responsible for late twentieth century O_2 variability in the North Pacific. Thermocline O_2 changes exhibit complex spatiotemporal patterns that are associated with changes in both ideal age and export production, making the relative causes difficult to quantitatively attribute. In order to understand what O_2 changes reveal about the impact of climate variability on ocean biogeochemistry, we need to determine what processes are responsible for the dominant O_2 anomalies.

4. Discussion

4.1. Attribution

[29] We perform two additional simulations in which individual causes of O_2 variability are successively removed, allowing us to isolate and characterize the contribution of ventilation, circulation, and biology to total O_2 changes. We begin by considering AOU along an isopycnal surface, which can be written as the sum of a "preformed" value, AOU_o, defined just below the mixed layer, and the total O_2 consumption since the water left contact with the mixed layer,

$$AOU = AOU_o + \oint OUR * ds/v, \quad (1)$$

where OUR is the O_2 utilization rate, which is integrated along each displacement, ds, of the water parcel as it is transported with velocity, v. The second term on the right-hand side therefore integrates the spatially and temporally varying O_2 consumption along the path of the circulation, whose direction and speed are also spatially and temporally variable.

[30] Preformed AOU is defined at each grid point where an isopycnal layer intersects the mixed layer. This is because while mixed layer O_2 is fixed at its saturated value (AOU = 0), the AOU on an isopycnal surface lying just below the mixed layer depends on the degree of exchange with (i.e., ventilation by) the mixed layer. If the detrainment of waters from the winter mixed layer onto an isopycnal surface is large, AOU_o will be brought close to zero. If the mixed layer is relatively isolated from the underlying isopycnal surface, the preformed AOU could be much larger than zero.

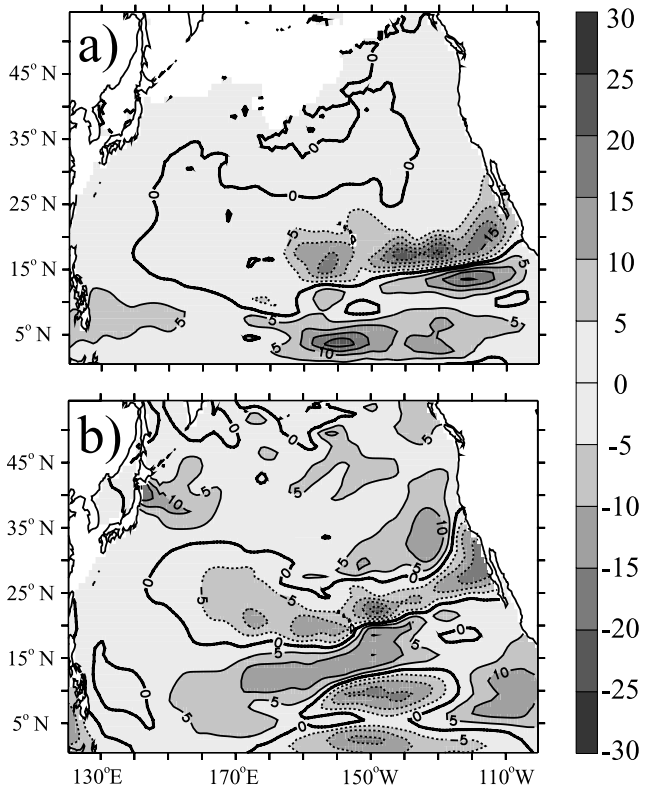

Figure 6. Change in ideal age in years, defined as the time since a water parcel was last in the mixed layer, from the 1980s to the 1990s for (a) σ_θ 25.8 and (b) σ_θ 26.6. Positive values indicate increasing ideal age with time.

[31] From equation (1) we can see that changes in AOU can be caused by changes in its preformed value (AOU_o), changes in OUR, or changes in the speed (v) or pathway (ds) of circulation. These contributions to total AOU change can be written schematically as

$$\begin{aligned}\Delta AOU &= \Delta AOU_o + OUR * \Delta circ + \Delta OUR * circ \\ &= \Delta AOU_{vent} + \Delta AOU_{circ} + \Delta AOU_{bio}. \end{aligned} \quad (2)$$

The first term on the right-hand side (ΔAOU_o) represents a change in preformed AOU and is therefore associated with changes in the transfer of O_2-rich waters across the base of the mixed layer. We refer to this term as a "ventilation AOU change" (ΔAOU_{vent}). The second term represents an AOU anomaly caused by a change in the circulation (Δcirc), which transports water masses along altered paths (or with altered rates) through the climatological OUR field. We refer to this term as the "circulation AOU change" (ΔAOU_{circ}) since it is due to the direct affect of changes in water mass location and transport. The last term represents the integrated AOU anomaly due to a change in the distribution of OUR. We refer to this as a "biological AOU change" (ΔAOU_{bio}). It is worth noting that changes in OUR can be caused by both changes in export flux and by changes in the depth of an isopycnal surface.

[32] Individual sources of AOU variability can now be quantified by performing model integrations in which various terms in equation (2) are eliminated. In order to remove biological AOU changes, we perform a second model integration with the same variable circulation, but this time using the climatological (monthly varying) OUR field diagnosed from the equilibrium spin-up. Holding the pattern of OUR constant through time on each isopycnal surface removes the affect of changes in biological O_2 consumption, leaving only ventilation and the direct circulation effects as factors in the variation of O_2/AOU.

[33] In a third simulation, we remove the influence of both ventilation and biological changes on O_2/AOU values by holding both OUR and AOU_o constant at their climatological values. Changes in AOU_o are removed by forcing the AOU on each isopycnal surface to remain at its monthly climatological value wherever that surface intersects the mixed layer either in the climatological mean state or at any time during the variable circulation run. For example, the region in which a given isopycnal surface intersects the mixed layer could shift poleward as a result of warming. This would produce a new region of isopycnal/mixed layer interaction to the north of the climatological outcrop. The effect of increased ventilation on O_2/AOU in that region is eliminated in this simulation, by forcing AOU at the local isopycnal/mixed layer interface to remain at climatological values. Similarly, equatorward of the climatological outcrop the isopycnal layer will lose contact with the mixed layer, as less dense water intercedes between them. The impact on O_2 of the resulting decrease in ventilation is again prevented, by maintaining the AOU at its climatological value at that location. This manipulation removes the effect of changes in the location and/or strength of ventilation, assuring that changes in the detrainment of mixed layer water onto an isopycnal surface will have no effect on the preformed AOU. Holding constant both OUR and AOU_o therefore yields AOU changes that result solely from the direct influence of circulation changes.

[34] Table 1 summarizes the three simulations and the sources of AOU variability in each one. The contribution of biology, ventilation, and circulation to the total AOU change can thus be separated as follows:

$$\Delta AOU_{circ} = \Delta AOU(\text{Experiment 3}),$$
$$\Delta AOU_{vent} = \Delta AOU(\text{Experiment 2}) - \Delta AOU(\text{Experiment 3}),$$
$$\Delta AOU_{bio} = \Delta AOU(\text{Experiment 1}) - \Delta AOU(\text{Experiment 2}).$$

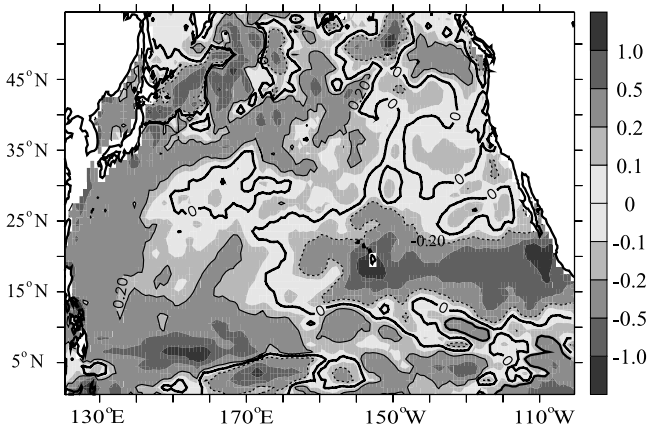

Figure 7. Difference in export flux between the 1980s and 1990s, as a fraction of the mean local value in those decades.

Table 1. Summary of Simulations Used to Isolate Components of Model AOU Variability[a]

Experiment	Description	AOU Terms Present
1	full variability	$\Delta AOU_{bio} + \Delta AOU_{vent} + \Delta AOU_{circ}$
2	climatological OUR field	$\Delta AOU_{vent} + \Delta AOU_{circ}$
3	climatological OUR field, and climatological preformed AOU	ΔAOU_{circ}

[a]See section 4.1 for details.

The sum of AOU anomalies from these three processes yields the total AOU change. Finally, we note that because the ventilation and circulation of the thermocline are dynamically coupled processes it is impossible to strictly separate their impacts on O_2 distributions. What we seek instead is an approximation of the direct role of each process, which must be evaluated a posteriori for consistency with basic features of ocean circulation (e.g., ventilation-induced O_2 changes should originate in regions where ventilation occurs) and related patterns of model variability (e.g., biologically induced O_2 changes should resemble patterns of export flux anomalies).

[35] The contributions of biology, circulation, and ventilation changes to the simulated O_2 difference between the 1980s and the 1990s are shown in Figures 8 and 9. Each map represents the contribution to the decadal O_2 difference of a single process integrated along the path of circulation since the beginning of the simulation. For example, the ventilation O_2 change between the 1980s and 1990s includes not only the local effect at the outcrop location of ventilation changes occurring in those 2 decades, but the affect of ventilation changes from 1948 to 1990 throughout the basin. For this reason, a ventilation O_2 change may be observed far from the isopycnal outcrop, corresponding to changes in the more distant past that have been transported and dispersed by the circulation. The sum of the O_2 changes attributed to all three processes, together with the small change in O_2^{sat}, is equal to the total O_2 difference over the specified period.

[36] On σ_θ 26.6, O_2 changes are predominantly caused by physical processes of circulation and ventilation. The direct impact of changes in circulation constitutes the largest source of O_2 changes in the tropical-to-subtropical latitudes, while ventilation is an important factor in much of the subpolar region. In the western subpolar gyre, ventilation changes are the primary cause of O_2 decreases. Decreased

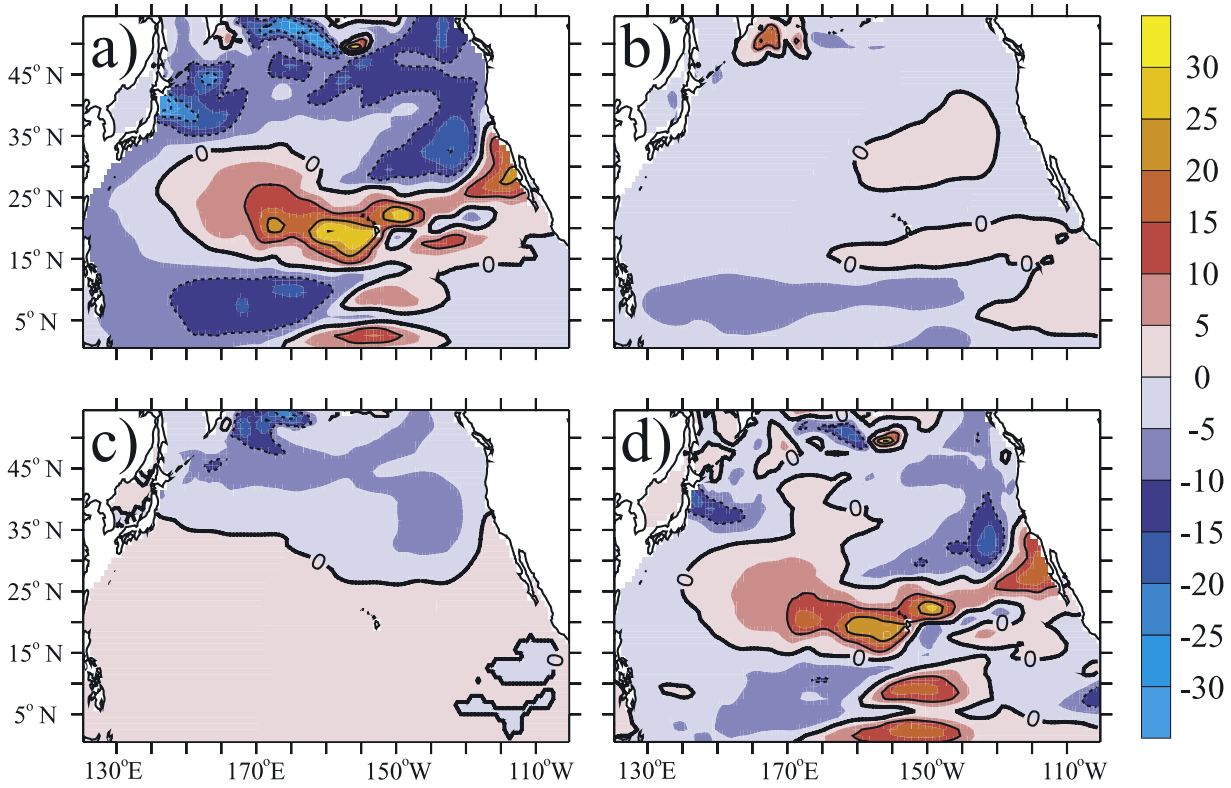

Figure 8. Difference between decadal mean O_2 (μmol/kg) in the 1990s and the 1980s along the isopycnal surface σ_θ 26.6. The (a) total O_2 difference is the sum of O_2 anomalies due to (b) biological changes, (c) ventilation changes, (d) changes in circulation, and thermodynamically driven O_2 changes, which are negligible (not shown). The decadal O_2 difference is nearly equal to but opposite of the total decadal AOU change.

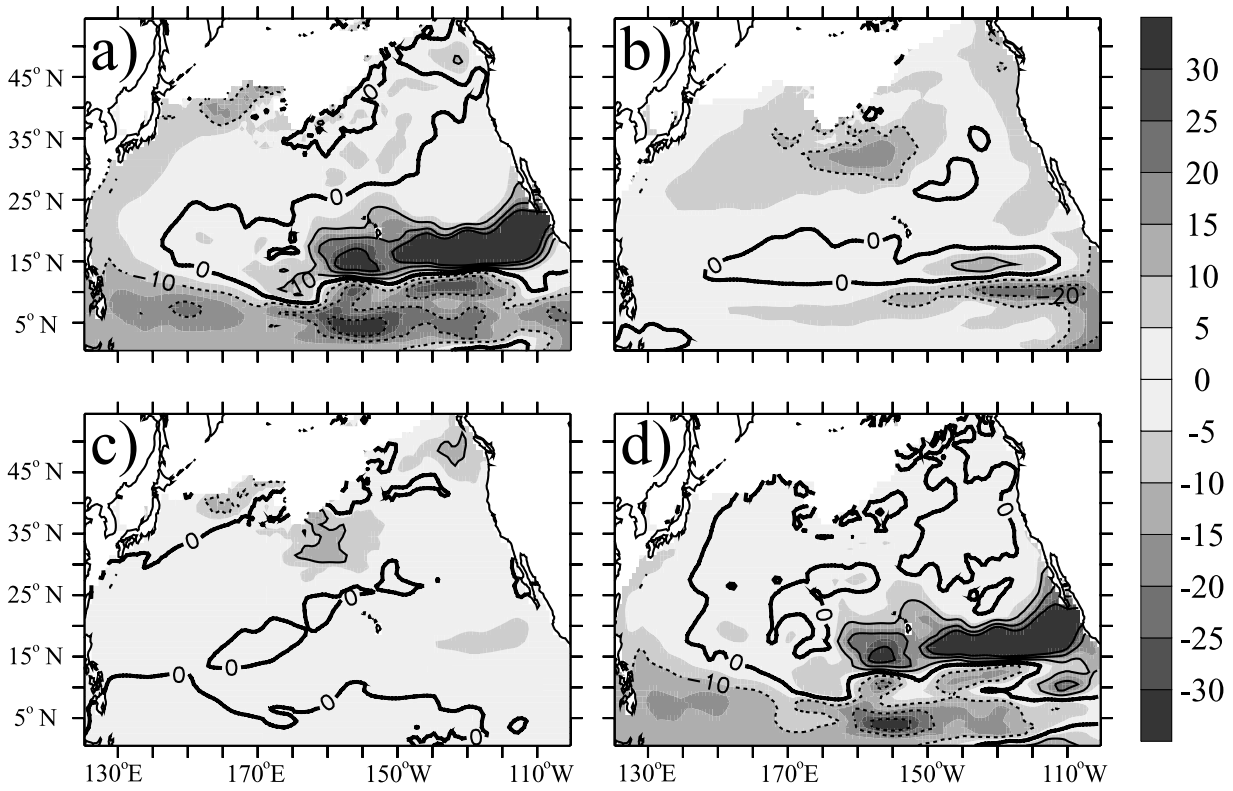

Figure 9. Same as Figure 8, but for isopycnal layer σ_θ 25.8.

O_2 in the northeastern Pacific is caused roughly equally by changes in ventilation and circulation. The effect of reduced ventilation may still be underestimated, however, because the model does not account for changes in surface fresh water forcing. The salinity of North Pacific Intermediate Water has been shown to have decreased during recent decades [*Wong et al.*, 1999a]. The freshening of surface waters in this region would increase the stratification of the upper water column, likely amplifying the reduction in ventilation and the associated AOU increase in the model's subpolar region. The large band of increased O_2 extending across the subtropical gyre is almost entirely circulation driven. O_2 changes attributable to biology are very small (<5 μM), except in the tropics and in a small region of the Subarctic North Pacific, where biological anomalies are an important part of the total O_2 change. Changes in O_2^{sat} are insignificant ($\ll$5 μmol/kg) everywhere except in a narrow region off the east coast of Japan, where temperature gradients are large.

[37] In the central mode water (σ_θ 25.8, Figure 9) the response of O_2 to ventilation changes is spatially complex and includes both O_2 decreases along the Kuroshio Extension and positive anomalies across much of the rest of the northern basin. These ventilation-induced O_2 changes reflect changes in the ventilation rate of Central Mode Water that are positive in some regions and negative in others [*Ladd and Thompson*, 2002]. Circulation related O_2 changes are confined to the tropics, where O_2 concentrations decrease from the 1980s to the 1990s to the south of 10°N, but increase north of 10°N. Biologically induced O_2 changes are more important on this density surface, where decadal differences in excess of 10 μM occur in several regions. Decreased O_2 in an eastern tropical band along 10°N and in the subtropical-subpolar transition zone (30°N–40°N) correspond to regions of increased export from the 1980s to the 1990s, while reduced export along ~15°N allows O_2 to increase in underlying waters (Figure 10).

[38] Because most of the remineralization of sinking organic matter occurs above 300 m, the impact of biological variability on O_2 is concentrated in the shallow water column. The strong decrease in sinking flux with depth also means that the signature of export changes on thermocline O_2 is spread across many isopycnal surfaces. Export anomalies in the center of the subtropical gyre, where isopycnals are deep, are seen primarily on light density surfaces, whereas a tropical export change affects O_2 on denser surfaces as well (see Figures 8b and 9b). For this reason, O_2 changes observed along constant density surfaces bear only a weak resemblance to surface productivity changes, even when productivity changes are significant. When biological O_2 anomalies are plotted on constant depth surfaces (not shown), they are seen to closely match the pattern of export changes.

[39] While biologically driven O_2 changes on σ_θ 25.8 are significant, they are offset to a large degree by physically driven anomalies. For example, the widespread biological O_2 decreases in the central North Pacific are roughly balanced in that region by increased O_2 due to circulation and ventilation. The close coupling of biologically and physically driven O_2 variability is due to the biological compensation mechanism discussed above, in which an

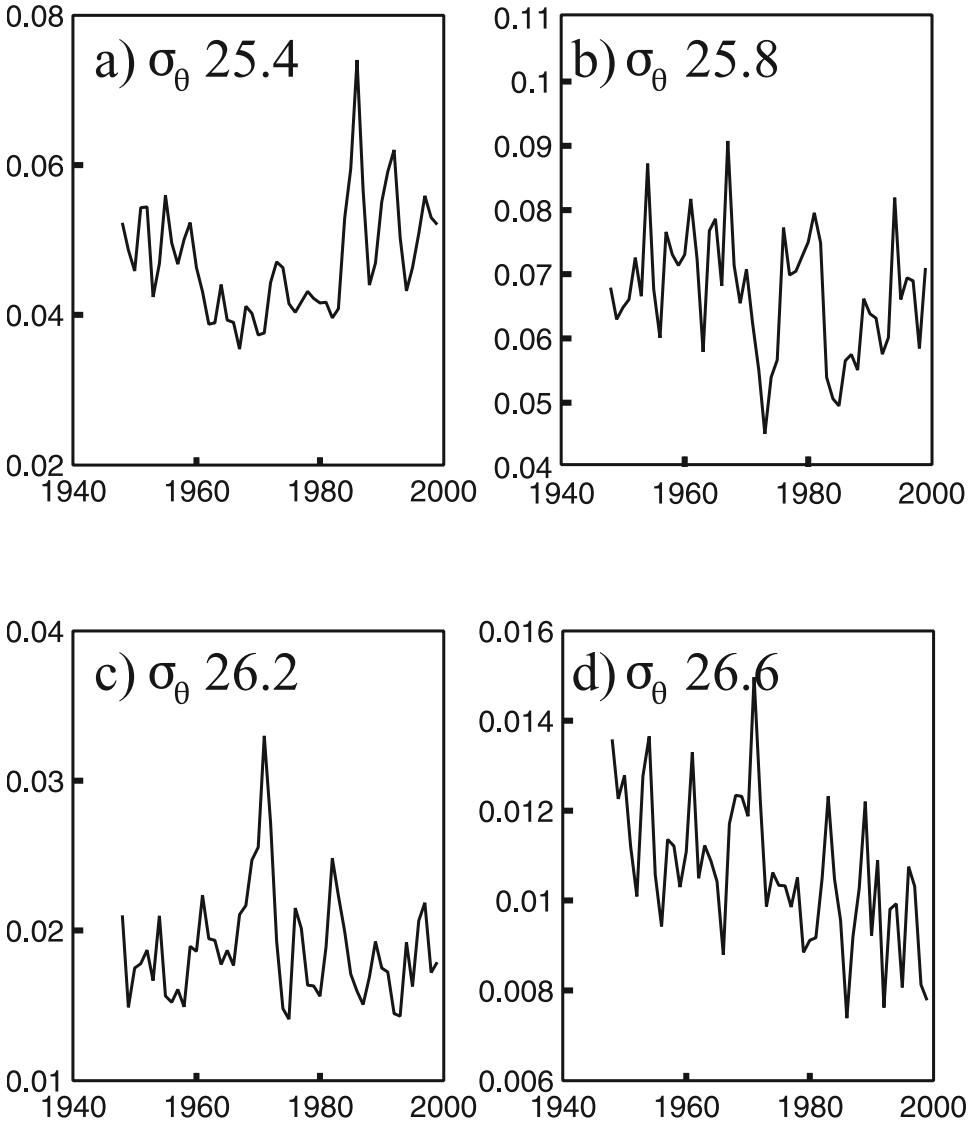

Figure 10. Ventilation rates from 1948 to 2000 on isopycnal layers (a) σ_θ 25.4 representing subtropical mode water, (b) σ_θ 25.8 and (c) σ_θ 26.2 representing central mode water, and (d) the base of the ventilated thermocline (σ_θ 26.6). Rates are given as a mean detrainment velocity of waters from the winter mixed layer onto the isopycnal layer.

increase in O_2 supply to the ocean interior is accompanied by an overall increase in nutrient supply back to the surface layer. If such changes in nutrient supply are not balanced by changes in organic matter export, as assumed in our model, this coupling could be weaker than suggested by our results. Nevertheless, unless organic matter export is completely decoupled from changes in nutrient supply, O_2 trends that arise from changes in the biological pump are likely to be difficult to detect owing to counteracting physically driven O_2 changes. A better understanding of historical changes in surface nutrient concentrations would help to constrain the strength of biological-physical compensation in the variability of thermocline O_2.

4.2. Origins of ΔAOU_{vent} and ΔAOU_{circ}

[40] The attribution of simulated O_2 changes indicates that ventilation and circulation are the dominant drivers of lower thermocline O_2 variability in the late twentieth century. Here we trace the origins of the primary O_2 anomalies to specific changes in lower thermocline ventilation and circulation. We find that O_2 differences between the 1980s and 1990s are due to both decadal trends in ventilation and circulation, and to episodic physical perturbations that generate large-scale propagating O_2 anomalies with decadal lifetimes.

[41] Ventilation rates among different isopycnal layers respond differently to atmospheric forcing (Figure 10). All layers, however, exhibit significant interannual variability over the course of the hindcast simulation. On σ_θ 26.6, ventilation rates decrease throughout the simulation, owing largely to a reduction in the area of the wintertime outcrop. This reduces the flux of well-oxygenated waters onto this isopycnal, causing O_2 decreases from the 1970s through the 1990s (Figure 5). The reduced outcrop area of denser

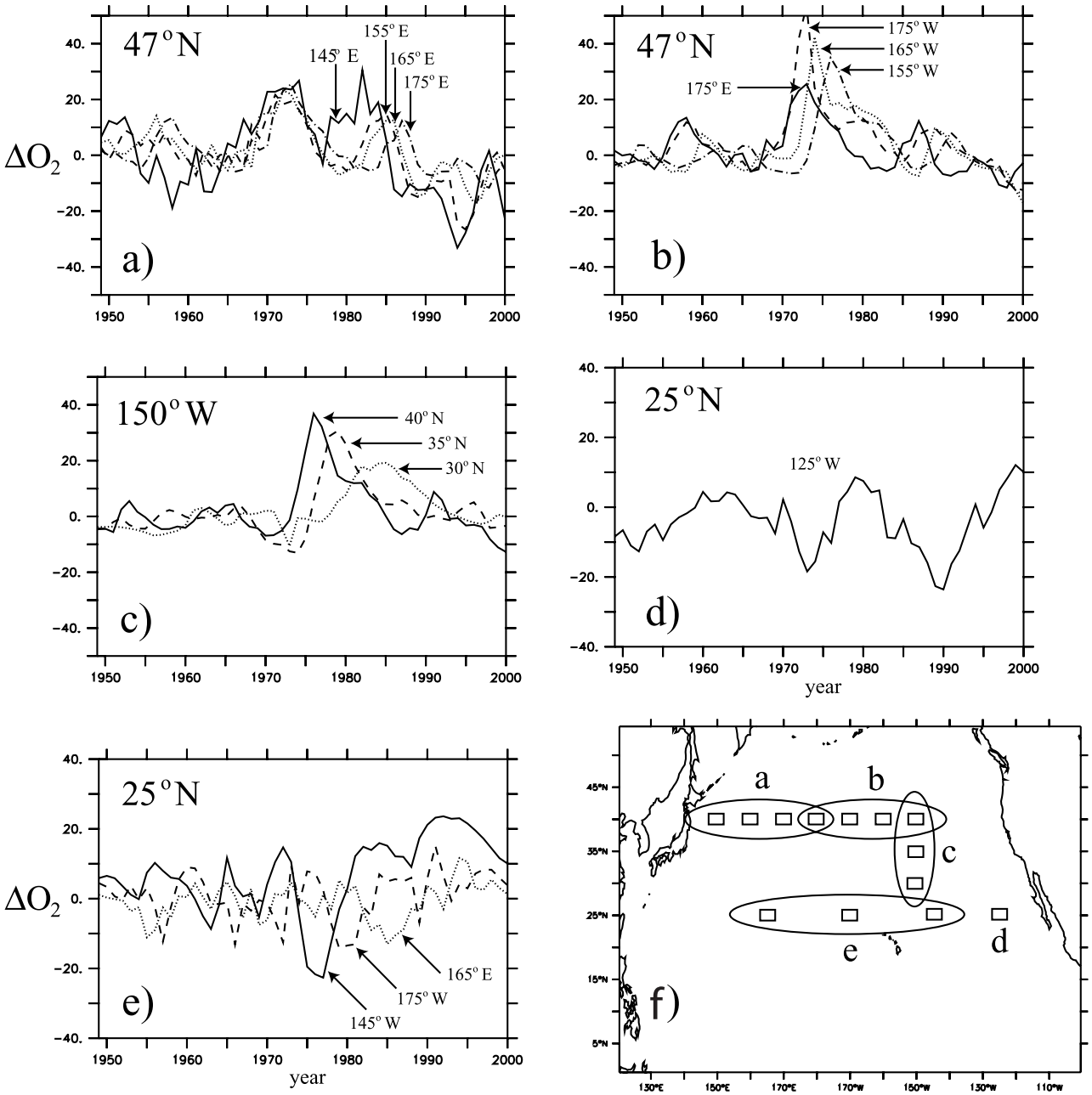

Figure 11. Time series of O_2 concentrations (minus the mean value during the 1960s) at locations in the subtropical North Pacific showing the propagation of anomalies (a, b) from the Kuroshio/Oyashio Extension and (d) from the eastern tropical North Pacific into (c, e) the subtropical gyre. In each case, the O_2 anomaly originates in the early 1970s, but remains an identifiable feature into the 1990s. (f) Locations of the time series given in Figures 11a–11e.

isopycnals is compensated by an increase in the area of outcropping among shallower isopycnals, whose wintertime outcrops expand northward. The increase in outcrop area, together with intensified wind speeds in the northwest Pacific leads to enhanced overall ventilation rates from the 1970s to the 1990s (Figure 10a) among subtropical mode waters ($\sigma_\theta < 25.8$).

[42] While decadal changes in ventilation rate account for much of the O_2 decrease in the subarctic Pacific below σ_θ 26.0, decadal circulation changes account for much of the subtropical O_2 increases. The origin of this simulated decadal O_2 change is a southward expansion of the subtropical gyre from the 1980s to the 1990s, causing low-O_2 waters in the North Equatorial Countercurrent to be displaced along ~15°N–20°N by relatively well oxygenated waters in the gyre's North Equatorial Current lying just to the north. The observed O_2 changes along 152°W south of 25°N (Figure 4), together with concurrent salinity changes [*Emerson et al.*, 2001], support such an expansion of the subtropical gyre.

[43] Circulation related O_2 changes are also observed in the Kuroshio/Oyashio Extension (KOE) region, where

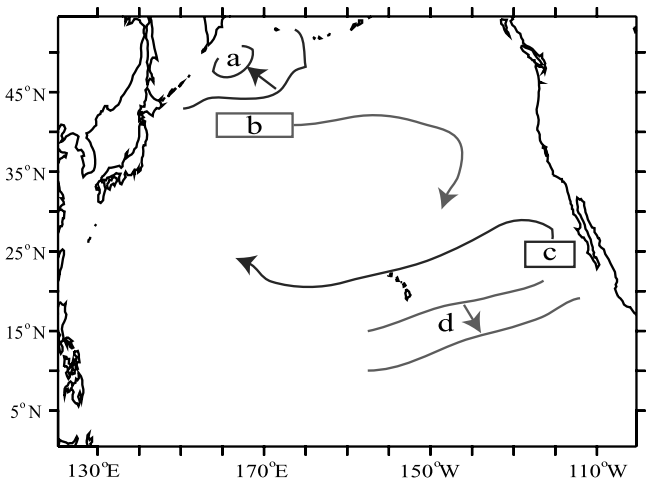

Figure 12. Schematic summary of the origins of major O_2 changes from the 1980s to the 1990s in the lower ventilated thermocline. The physical causes of anomalies labeled a through d are identified in Table 2 and described in the text.

strong meridional O_2 gradients are produced by the confluence of warm tropical/subtropical waters of the Kuroshio current and cold subpolar waters of the Oyashio current. The position of the model KOE oscillates narrowly between a more northern and southern location. Fluctuations in both the strength and position of the Kuroshio Extension produce decadal O_2 deviations throughout the simulation (Figure 11a). Some shifts occur along the entire current, causing simultaneous O_2 changes from the western boundary to the central Pacific (e.g., early 1970s, Figure 11a). Other shifts, for example in the late 1970s, are focused in the western boundary, where the O_2 anomalies are generated and transported eastward (Figure 11a). The timing and western intensification of this shift in the Kuroshio Extension, coincident with the well-known shift in the Pacific Decadal Oscillation, are features that have been observed in historical hydrographic data [*Deser et al.*, 1999].

[44] Decadal changes in circulation and ventilation explain much of the O_2 anomaly pattern, but shorter-term episodic events also contribute substantially to O_2 variability. Some physical perturbations generate O_2 anomalies of sufficient scale and intensity that they remain coherent features for over a decade. Such anomalies are capable of traveling far from their regions of origin, becoming progressively broader but lower in amplitude as they are transported across the basin (Figure 11c).

[45] For example, the multidecadal trend toward reduced ventilation of σ_θ 26.6 is punctuated by a brief period of increased O_2-rich mass flux in the early 1970s (Figure 10d), when a new region of ventilation opens in the central Pacific along 35°N–40°N. This ventilation event injects a large bolus of high O_2 water into the permanent thermocline (Figure 11b), adding to the elevated O_2 originating in the KOE. The high O_2 anomaly continues eastward and then southward into the subtropical gyre, producing first an increase in O_2 along 150° W from the 1970s to the 1980s (Figure 5) followed by a decrease from the 1980s to the 1990s. This transient response to the temporary increase in ventilation on σ_θ 26.6 contributes to the simulated O_2 decrease coincident with that observed by *Emerson et al.* [2001].

[46] Episodic physical perturbations also contribute to the model's subtropical O_2 increases. For example, the O_2 increase in the center of the gyre on σ_θ 26.6 is the remnant signal of a transient O_2 anomaly transported westward from the eastern tropical North Pacific (ETNP). In the early 1970s, low-O_2 waters carried north by the coastal California Undercurrent are briefly entrained into the broad, southward flowing California Current. The resulting mass of O_2-depleted water is carried into the subtropical gyre by the California and North Equatorial Currents (Figures 11d and 11e), causing first local O_2 decreases (e.g., west of Hawaii from the 1970s to the 1980s, Figure 7) followed by local O_2 increases (e.g., same region from the 80s to 90s, Figure 6) as the anomaly is transported through the region and O_2 levels return to their background levels. Evidence for the presence of low -O_2 water masses originating in the ETNP has been observed near Hawaii by [*Lukas and Santiago-Mandujano*, 2001].

[47] To summarize, the differences in O_2 between the 1980s and 1990s at the base of the ventilated thermocline are caused by a combination of decadal trends in circulation and ventilation, and transient responses to brief, localized physical perturbations (Figure 12 and Table 2). In the subpolar region, O_2 decreases on σ_θ 26.6 are due to a multidecadal reduction in lower thermocline ventilation rates. In the subtropics, O_2 increases at the southeastern gyre boundary are due to the southern expansion of the gyre from the 1980s to the 1990s. At the subtropical/subpolar transition zone, a large positive O_2 anomaly is generated in the early 1970s by a displacement of the Kuroshio Extension and the brief onset of ventilation in the central Pacific. At the same time, a bolus of low-O_2 water is

Table 2. Specific Physical Causes of Simulated Decadal O_2 Changes Between the 1980s and 1990s on Isopycnal σ_θ 26.6[a]

ΔO_2 (1990s–1980s) on σ_θ 26.6	Ventilation	Circulation
Decadal trends	subpolar O_2 decrease, Figure 12, label a	subtropical O_2 increase, Figure 12, label d
Interannual perturbations	subtropical O_2 decrease (preceded by an increase, 1970s to 1980s), Figure 12, label b	subtropical O_2 increase (preceded by a decrease, 1970s to 1980s), Figure 12, label c

[a]Both episodic and sustained changes in both ventilation and circulation are found to account for major decadal O_2 anomalies. See Figure 12 for corresponding spatial summary.

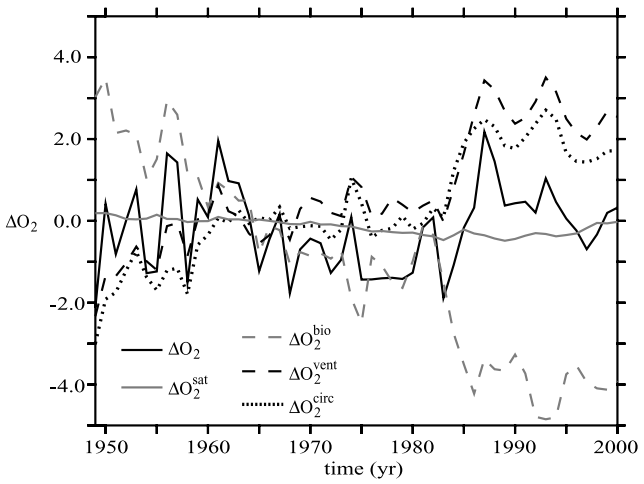

Figure 13. Changes in average O_2 concentrations relative to the 1960s, for the entire thermocline ($\sigma_\theta < 27.0$) of the model North Pacific basin. Mean O_2 anomalies (solid black line) are decomposed into contributions from changes in O_2 solubility (solid gray line), ventilation (dashed black line), circulation (dotted black line), biology (dashed gray line) according to equation (2). Biologically and physically driven O_2 changes act to maintain a constant O_2 inventory over the course of the simulation, although interannual variations of $\sim$5 μM are evident.

entrained into the California Current from the oxygen minimum zone in the east. Both of these anomalous water masses are subsequently transported into the gyre, causing regional trends in the 1970s to the 1980s that reverse sign into the 1990s as the anomaly is dissipated and transported out of the region.

4.3. Changes in O_2 Inventory

[48] The mean O_2 anomaly averaged over the entire basin thermocline from the base of the mixed layer to σ_θ 27.0 (Figure 13) reveals an interannual variability of $\sim$5 μM, but no long-term change during the course of the simulation. Thus the O_2 inventory of the North Pacific remains relatively stable over the period 1950–2000 despite the presence of significant regional trends. Using the separation of O_2 changes due to biological, ventilation and circulation, we can quantify the effect of each process on O_2 inventory.

[49] The response of the mean basin O_2 concentration due to variability in physical processes of circulation and ventilation is an increase of roughly 4 μM (Figure 13). The simulated expansion of the subtropical gyre into formerly suboxic waters of the ETNP accounts for at least part of the circulation-driven O_2 increase. The net effect of variable ventilation rates also enhances the supply of O_2, when averaged across the basin. Increased ventilation rates among shallower surfaces evidently dominate the reduced ventilation of the lower ventilated thermocline (σ_θ 26.6), the process responsible for significant subpolar O_2 decreases. Why do we not see large O_2 increases in the shallow thermocline associated with the increased ventilation rates?

[50] The intensification of North Pacific circulation causes an increasing supply of nutrients to the surface and therefore an increase in subsurface biological O_2 consumption. The resulting biological O_2 anomalies averaged over the entire basin decrease with time and closely compensate the combined anomalies due to ventilation and circulation, thus stabilizing the total O_2 burden on the decadal timescale. The coupling of biological and physical O_2 changes is seen regionally on σ_θ 25.8 (Figure 9). In the central North Pacific, regions of enhanced ventilation are often coincident with increased biological O_2 consumption due to elevated export flux. In the absence of changes in biological productivity, physically driven O_2 changes would therefore be observed throughout the water column. Instead, physically driven changes are largely compensated by biologically driven O_2 changes in the shallow water column, where oxygen utilization rates are relatively high. In contrast, the lower ventilated thermocline experiences relatively low rates of O_2 consumption, and physically driven O_2 variability remains largely uncompensated.

[51] The close coupling of biologically and physically driven O_2 variability is in part a consequence of maintaining constant surface nutrients. In the absence of a change in surface nutrients, it is sea surface temperatures (i.e., the thermodynamic boundary condition for O_2 saturation; see Figure 13) that govern the O_2 inventory. In the absence of changes in surface nutrients and SST, the O_2 content of the ocean interior cannot change for more than a few years.

5. Conclusions

[52] We describe and analyze the temporal evolution of O_2 in the shallow water column of the North Pacific simulated with a hindcast model of physical-biogeochemical variability. The simulated response of oceanic O_2 to historical climate change in the North Pacific involves complex spatial and temporal changes, rather than constant, basin-wide trends. Consistent with observations, the model predicts decreased O_2 in the lower ventilated thermocline at subpolar latitudes and increased O_2 over much of the subtropics between the 1980s and 1990s. While the magnitudes of decadal O_2 differences appear to be generally underestimated by the model, especially in the subpolar region, the overall pattern of changes is consistent with observations, suggesting that the model reproduces important modes of physical-biogeochemical variability.

[53] In the lower ventilated thermocline, where observed O_2 changes are strongest, O_2 variability is dominated by physical processes of ventilation and circulation. A long-term reduction in the ventilation of the densest waters outcropping in the open northwest Pacific (σ_θ 26.6) leads to O_2 decreases throughout much of the subarctic basin from the 1970s through the 1990s. The amplitude of simulated O_2 decreases is weaker than that inferred from observations, which may indicate that changes in the hydrological cycle [*Wong et al.*, 1999a] not represented in the model also play an important role in the suppression of lower thermocline ventilation in the late twentieth century. Changes in O_2 due to circulation are most pronounced at the boundaries of the subtropical gyre, where decadal shifts in the mean position of major currents such as the Kuroshio Extension and the NECC produce strong O_2 changes at the gyre edges.

[54] Episodic physical perturbations also contribute to significant decadal O_2 variability by generating large-scale

transient O_2 anomalies that are transported across the basin on a decadal timescale. A substantial portion of the subtropical O_2 difference between the 1980s and the 1990s can be traced to brief fluctuations in the rates or patterns of ventilation and circulation occurring in the early 1970s. These perturbations originate in the ETNP and Kuroshio Extension, regions with strong O_2 gradients that act as engines of subtropical O_2 variability.

[55] Decadal trends in biological export production driven by a variable nutrient supply are significant, but their impact on O_2 concentrations is confined to the shallow thermocline ($\sigma_\theta < 25.8$), owing to the strong decrease of organic matter oxidation with depth. In addition, changes in biological O_2 consumption often counteract physically driven changes in O_2 supply even on a regional scale, resulting in smaller net O_2 anomalies than would be predicted on the basis of export flux. This physical-biological coupling acts to stabilize the basin-wide O_2 inventory on the timescale of thermocline ventilation.

[56] These results have broad implications for the detection and attribution of climate-related changes in ocean biogeochemical processes. The presence of large-scale propagating O_2 anomalies with decadal lifetimes complicates the detection of long-term trends in oceanic O_2 associated with anthropogenic climate change. This is especially true for the subtropics, which appear to be strongly influenced by transient anomalies generated by episodic physical perturbations. Decadal-scale changes in biological export production may be difficult to detect on the basis of O_2 alone owing to the compensation between physically and biologically driven O_2 changes. In the lower thermocline however, O_2 appears to be a reliable tracer of decadal changes in the circulation and ventilation. Continued analysis of historical O_2 data will help to determine whether O_2 changes observed in these water masses over the past couple decades in the North Pacific are associated with decadal climate variability or reflect longer term anthropogenic climate change.

Appendix A

[57] In order to compare simulated O_2 variability on interannual and longer timescales to the observations, we need to account for the effect of seasonal O_2 variations among measurements made during different months as well as different years. Along 152°W, *Emerson et al.* [2001] found that while seasonal O_2 variations may be significant, they could not account for the phasing of O_2 changes inferred from four repeat cruises examined. We have attempted to evaluate the potential for seasonal O_2 variability to contribute to observed O_2 differences along 47°N and 165°E using the monthly World Ocean Atlas climatology (Figure A1). We find that seasonal variations in O_2 along 47°N can be quite strong, with values up to 50 μM. However, seasonal anomalies are zonally heterogeneous and do not extend across the basin, possibly reflecting strong wave propagation along the Kuroshio Extension. When averaged across 47°N, thermocline O_2 variability is therefore greatly attenuated. This suggests that while the local magnitude of observed O_2 differences along 47°N may be affected by seasonal O_2 variability, the overall decrease is likely to reflect longer-term changes. In addition, the continuity of O_2 differences at the intersections of the cruise transects, each of which would contain a different seasonal contribution, requires that the changes are at least partly interannual to interdecadal in nature.

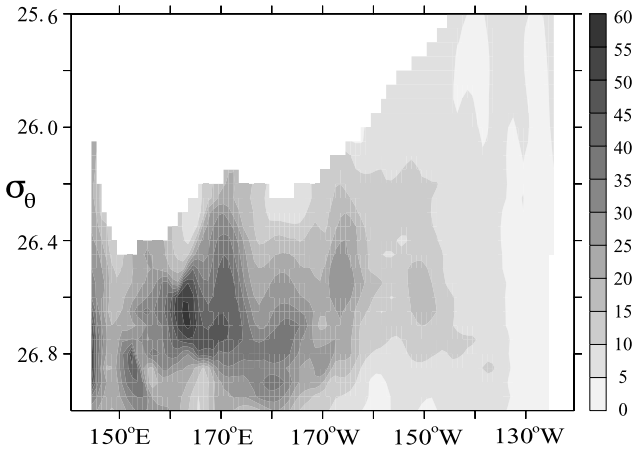

Figure A1. Standard deviation of climatological monthly AOU (μmol/kg) along 47°N, according to the World Ocean Atlas [*Conkright et al.*, 2001]. Monthly AOU variability, while large in amplitude, is not coherent across the basin.

[58] **Acknowledgments.** We thank Y. Watanabe and R. M. Key for making available the O_2 data from several cruises. C. D. was supported by a fellowship from the Program on Climate Change at the University of Washington. S. E. and L. T. were supported by grants from the U.S. National Science Foundation.

References

Anderson, L. A., and J. L. Sarmiento (1994), Redfield ratios of remineralization determined by nutrient data analysis, *Global Biogeochem. Cycles*, *8*, 65–80.

Bindoff, N. L., and T. J. McDougall (2000), Decadal changes along an Indian Ocean section at 32°S and their interpretation, *J. Phys. Oceanogr.*, *30*, 1207–1222.

Chavez, F. P., J. Ryan, S. E. Lluch-Cota, and M. C. Niquen (2003), From anchovies to sardines and back: Multidecadal change in the Pacific Ocean, *Science*, *299*, 217.

Conkright, M., S. Levitus, and T. Boyer (1994), *World Ocean Atlas 1994*, vol. 1, *Nutrients*, *NOAA Atlas NESDIS 1*, 16 pp., NOAA, Silver Spring, Md.

Deser, C., M. A. Alexander, and M. S. Timlin (1996), Upper-ocean thermal variations in the North Pacific during 1970–1991, *J. Clim.*, *9*, 1840–1855.

Deser, C., M. A. Alexander, and M. S. Timlin (1999), Evidence for a wind-driven intensification of the Kuroshio Current Extension from the 1970s to the 1980s, *J. Clim.*, *12*, 1697–1706.

Deutsch, C., S. Emerson, and L. Thompson (2005), Fingerprints of climate change in North Pacific oxygen, *Geophys. Res. Lett.*, *32*, L16604, doi:10.1029/2005GL023190.

Emerson, S., P. D. Quay, C. Stump, D. Wilbur, and R. Schudlich (1995), Chemical tracers of productivity and respiration in the subtropical Pacific Ocean, *J. Geophys. Res.*, *100*, 15,873–15,887.

Emerson, S., S. Mecking, and J. Abell (2001), The biological pump in the subtropical North Pacific Ocean: Nutrient sources, Redfield ratios, and recent changes, *Global Biogeochem. Cycles*, *15*, 535–554.

Emerson, S., Y. W. Watanabe, T. Ono, and S. Mecking (2004), Temporal trends in apparent oxygen utilization in the upper pycnocline of the North Pacific: 1980–2000, *J. Oceanogr.*, *60*, 139–147.

Garcia, H., A. Cruzado, L. Gordon, and J. Escanez (1998), Decadal-scale chemical variability in the subtropical North Atlantic deduced from nutrient and oxygen data, *J. Geophys. Res.*, *103*, 2817–2830.

Hallberg, R., and P. Rhines (1996), Buoyancy-driven circulation in an ocean basin with isopycnals intersecting the sloping boundary, *J. Phys. Oceanogr.*, *26*, 913–940.

Ito, T., M. Follows, and E. A. Boyle (2004), Is AOU a good measure of respiration in the oceans?, *Geophys. Res. Lett.*, *31*, L17305, doi:10.1029/2004GL020900.

Jenkins, W. J. (1990), Determination of isopycnal diffusivity in the Sargasso Sea, *J. Phys. Oceanogr.*, *21*, 1058–1061.

Johnson, G. C., and N. Gruber (2006), Decadal water mass variations along 20°W in the northeastern Atlantic Ocean, *Prog. Oceanogr.*, in press.

Kalnay, E., et al. (1996), The NCEP/NCAR 40-year reanalysis project, *Bull. Am. Meteorol. Soc.*, *77*, 437–471.

Karl, D., R. Letelier, L. Tupas, J. Dore, J. Christian, and D. Hebel (1997), The role of nitrogen fixation in biogeochemical cycling in the subtropical North Pacific Ocean, *Nature*, *388*, 533–538.

Keller, K., R. D. Slater, M. Bender, and R. M. Key (2002), Possible biological or physical explanations for decadal scale trends in North Pacific nutrient concentrations and oxygen utilization, *Deep Sea Res., Part II*, *49*, 345–362.

Ladd, C., and L. Thompson (2001), Water mass formation in an isopycnal model of the North Pacific, *J. Phys. Oceanogr.*, *31*, 1517–1537.

Ladd, C., and L. Thompson (2002), Decadal variability of North Pacific central mode water, *J Phys. Oceanogr.*, *32*, 2870–2881.

Ledwell, J. R., A. J. Watson, and C. S. Law (1993), Evidence for slow mixing across the pycnocline from an open ocean tracer release experiment, *Nature*, *364*, 701–703.

Levitus, S., and T. Boyer (1994), *World Ocean Atlas 1994*, vol. 4, *Temperature*, *NOAA Atlas NESDIS 4*, NOAA, Silver Spring, Md.

Lozier, M. S., M. S. McCartney, and W. B. Owens (1994), Anomalous anomalies in averaged hydrographic data, *J. Phys. Oceanogr.*, *24*, 2624–2638.

Lukas, R., and F. Santiago-Mandujano (2001), Extreme water mass anomaly observed in the Hawaii Ocean Time-series, *Geophys. Res. Lett.*, *28*, 2931–2934.

Matear, R. J., A. C. Hirst, and B. I. McNeil (2000), Changes in dissolved oxygen in the Southern Ocean with climate change, *Geochem. Geophys. Geosyst.*, *1*, doi:10.1029/2000GC000086.

McGillicuddy, D. J., R. Johnson, D. A. Siegel, A. F. Michaels, N. R. Bates, and A. H. Knap (1999), Mesoscale variations of biogeochemical properties in the Sargasso Sea, *J. Geophys. Res.*, *104*, 13,381–13,394.

McKinley, G. A., M. J. Follows, and J. Marshall (2004), Mechanisms of air-sea CO_2 flux variability in the equatorial Pacific and the North Atlantic, *Global Biogeochem. Cycles*, *18*, GB2011, doi:10.1029/2003GB002179.

Mecking, S., M. J. Warner, and J. L. Bullister (2006), Temporal changes in pCFC-12 ages and AOU along two hydrographic sections in the eastern subtropical North Pacific, *Deep Sea Res.*, in press.

Najjar, R., and J. C. Orr (1999), Biotic how-to, report, 15 pp., Lab. des Sci. du Clim. et de l'Environ./Comm. à l'Energie Atom., Gif-sur-Yvette, France.

Ono, T., T. Midorikawa, Y. W. Watanabe, K. Tadokoro, and T. Saino (2001), Temporal increases of phosphate and apparent oxygen utilization in the subsurface waters of western subarctic Pacific from 1968 to 1998, *Geophys. Res. Lett.*, *28*, 3285–3288.

Polovina, J. J., G. T. Mitchum, and G. T. Evans (1995), Decadal and basin-scale variation in mixed layer depth and the impact on biological production in the central and North Pacific, 1960–88, *Deep Sea Res., Part I*, *42*, 1701–1716.

Shaffer, G., O. Leth, O. Ulloa, J. Bendtsen, G. Daneri, V. Dellarossa, S. Hormazabal, and P. I. Sehlstedt (2000), Warming and circulation change in the eastern South Pacific Ocean, *Geophys. Res. Lett.*, *27*, 1247–1250.

Thiele, G., and J. Sarmiento (1990), Tracer dating and ocean ventilation, *J. Geophys. Res.*, *95*, 9377–9391.

Thompson, L., and C. A. Ladd (2004), The response of the North Pacific Ocean to decadal variability in atmospheric forcing: Wind versus buoyancy forcing, *J. Phys. Oceanogr.*, *34*, 1373–1386.

Venrick, E. L., J. A. Mcgowan, D. R. Cayan, and T. L. Hayward (1987), Climate and chlorophyll-a: Long-term trends in the central North Pacific Ocean, *Science*, *238*, 70–72.

Watanabe, Y. W., T. Ono, A. Shimamoto, T. Sugimoto, M. Wakita, and S. Watanabe (2001), Probability of a reduction in the formation rate of the subsurface water in the North Pacific during the 1980s and 1990s, *Geophys. Res. Lett.*, *28*, 3289–3292.

Wong, A. P. S., N. L. Bindoff, and J. A. Church (1999a), Large-scale freshening of intermediate waters in the Pacific and Indian oceans, *Nature*, *400*, 440–443.

Wong, C. S., F. A. Whitney, D. W. Crawford, K. Iseki, R. J. Matear, W. K. Johnson, and J. S. Page (1999b), Seasonal and interannual variability in particle fluxes of carbon, nitrogen and silicon from time series of sediment traps at Ocean Station P, 1982–1993: Relationship to changes in subarctic primary productivity, *Deep Sea Res., Part II*, *46*, 2735–2760.

C. Deutsch, S. Emerson, and L. Thompson, School of Oceanography, University of Washington, 407 OSB, Box 355351, Seattle, WA 98195-5351, USA. (cdeutsch@ocean.washington.edu)